Current Applied Physics 15 (2015) 110–114

Contents lists available at ScienceDirect

Current Applied Physics

journal homepage: www.elsevier.com/locate/cap

Silver-enhanced conductivity of magnetoplasmonic nanochains

Van Tan Tran [a], Hongjian Zhou [a], Jung Youn Park [b], Jongman Kim [c], Jaebeom Lee [a, *]

[a] Department of Cogno-Mechatronics Engineering, Pusan National University, Busan 609-735, Republic of Korea
[b] Department of Biotechnology Research, National Fisheries Research and Development Institute, Busan 619-706, Republic of Korea
[c] Department of Nano Fusion Technology, Pusan National University, Miryang 627-706, Republic of Korea

ARTICLE INFO

Article history:
Received 27 October 2014
Received in revised form
28 November 2014
Accepted 28 November 2014
Available online 28 November 2014

Keywords:
Fe_3O_4@Au nanoparticles
Nanochains
Self-assembly
Magnetoplasmonic
Silver enhancement

ABSTRACT

A method for improving the electrical properties of one-dimensional conducting structures by reductive deposition of metallic silver on a gold surface is presented. Fe_3O_4@Au core–shell nanoparticles were used to fabricate conducting magnetoplasmonic nanochains (MPNCs) through magnetic-field-induced assembly. The MPNCs were prepared on a solid substrate. Their dimension was controlled by adjusting the pH of the colloidal solution. The nanochains (NCs) were placed across gold microelectrodes, and additional metal was deposited by highly specific chemical enhancement of the colloidal gold using a silver enhancement solution. Silver-enhanced MPNCs show a remarkable morphology and an impressive enhancement in electrical properties compared to the as-prepared MPNCs.

1. Introduction

One-dimensional (1-D) nanostructured materials (e.g., nanowires, nanorods, and nanochains) have received much attention to date. These structures have been seen rapid development in recent years and emerged as powerful building blocks for numerous applications, such as nanoelectronics [1], optoelectronics [2], as well as electrochemical and biosensor devices [3,4]. In particular, conducting nanowires are attracting increasing attention because of their unique electrical properties and potential for the fabrication of high-performance devices [5–7]. Various techniques have been proposed to produce the 1-D conducting structures, including nano-imprint lithography [8], dip-pen [9], and template-based electrochemical deposition [10]. However, these conventional methods require sophisticated systems and/or complex processes. As an alternative, unconventional methods based on self-assembly of nanoscale units represent a fascinating strategy for the fabrication of 1-D structures with easily controllable dimensions and properties.

Alignment of magnetic colloidal nanoparticles (NPs) in suspension using an external magnetic field offers an interesting avenue to generate nanowires in a liquid matrix. Typically, magnetite NPs in suspension can be manipulated by an external magnetic field [11]. The structure of magnetic-based systems is determined by the interplay between interparticle features (e.g., shape, size, surface layer, magnetic dipole moment, etc.) and external stimuli. In the absence of an external magnetic field, isotropic Van der Waals forces are expected to play a dominant role in determining the colloidal stability of the nanoparticles. However, in the presence of a magnetic field, anisotropic magnetic dipole interactions can play a significant role in controlling the formation of chain-like structures along the magnetic field direction [12]. In order to produce conducting 1-D structures through magnetic-field-induced alignment, magnetic NPs must be covered with conducting materials. Conducting polymers have been reported as good candidates for this purpose because of their controllable chemical and electrochemical properties [13,14]. However, the main disadvantages are their relatively low stability and their insolubility in common organic solvents.

Recently, magnetic NPs covered with a thin gold or silver film attracted considerable interest because of their hybrid magnetic, plasmonic, and electrical properties. The corresponding materials are labeled magnetoplasmonic NPs (MPNPs). Our group reported magnetoplasmonic (Fe_3O_4@Au) core–shell NPs that consist of an Fe_3O_4 core and an Au shell [15]. Coating an Au layer on a magnetic core could preserve the chemical stability as well as the magnetic properties of Fe_3O_4. Additionally, the Au shell provides unique plasmonic and electric properties to the material, which is expected

* Corresponding author.
E-mail address: jaebeom@pusan.ac.kr (J. Lee).

http://dx.doi.org/10.1016/j.cap.2014.11.013
1567-1739/

to result in attractive applications in electronics and optics. As an example, we proposed a method to fabricate conducting NCs of Fe_3O_4@Au core–shell NPs utilizing the driving force of an external magnetic field [16]. After annealing treatment, these NCs were used as a transducer for DNA detection. Here, we introduce an alternative method for greatly improving the conductivity of NCs using silver enhancement. A six-fold improvement was found for the conductivity of MPNCs compared to annealed ones. The present study thus introduces a potential technique for the development of novel components for nanoelectronics, optoelectronics, and biosensors.

2. Experimental details

2.1. Materials

Sodium citrate ($Na_3C_6H_5O_7$), silver nitrate ($AgNO_3$), and hydroquinone ($C_6H_6O_2$) were obtained from Sigma–Aldrich Korea Ltd. (Yongjin, South Korea). Citric acid ($C_6H_8O_7$) was purchased from Hayashi Pure Chemical Ind., Ltd. (Japan). The deionized H_2O (18.2 mΩ/cm) used in most experiments was obtained from Human Corporation, South Korea. All chemicals were of analytical grade and used as received.

2.2. Fabrication silver-enhanced MPNCs

Fe_3O_4@Au NPs were synthesized according to our previously-developed method [17]. The 1-D MPNCs were obtained via external magnetic force as reported in ref. [16] (Fig. 1). The MPNCs were developed using a silver enhancement solution according to the previous literature [18,19]. First, a citrate buffer solution (pH 3.6) of hydroquinone was prepared by dissolving 0.1 M citric acid, 0.1 M trisodium citrate dehydrate, and 0.1 M hydroquinone in deionized water. The silver enhancement solution was made by mixing 1.7 ml of the buffer solution with 0.3 ml silver ion solution (0.1 M $AgNO_3$). The as-prepared MPNCs were incubated with the enhancement solution for 20 min under low light. The sample was then washed with deionized water and dried under nitrogen gas.

2.3. Microfabrication of electrode

The electrode was fabricated from a 4-inch silica wafer (thickness 0.5 mm). Photolithography was used to pattern photoresist. Metal electrodes were deposited by evaporation of 30 nm of chromium (for adhesion) under 100 nm of gold, and a lift-off process was used to develop the electrode. Each electrode finger had a length of 900 μm, a width of 100 μm and an in-between spacing of 5 μm. Electrode wafers were then cut into 1.2 cm × 1.1 cm chips with a dicing saw.

2.4. Characterization

The morphologies and sizes of the Fe_3O_4@Au NPs and MPNCs were characterized by HR-TEM (JEOL, JEM-3010, Japan), FE-SEM (S-4700, Hitachi, Japan), optical microscopy (DM2000, Leica, Germany), and AFM (Veeco diInnova, USA). Furthermore, their surface potential was monitored using a zeta-sizer (Malvern Instruments, ZS Nano, UK). The conductivity of the aligned MPNCs was measured by IviumStat (Ivium Technologies, The Netherlands).

3. Results and discussion

3.1. Control of MPNPs assembly

Fe_3O_4@Au NPs with diameter of 20 nm (10 nm Fe_3O_4 core, 5 nm Au shell) were synthesized in an aqueous solution according to our previous work [17]. It was reported that magnetic NPs dispersed in solution are generally subjected to two major types of forces: van der Waals (vdW) and magnetic dipolar interactions [20]. In our previous study, the dimension of MPNCs was controlled by varying the strength of the magnetic field, $|\boldsymbol{B}|$ which governs the magnetic dipolar interactions [16]. Here, we additionally explore the role of vdW interactions in the assembly of NPs by varying the pH of the colloidal solution. Fig. 2 shows microscopic images of MPNCs prepared from different pH solutions with the same applied magnetic field ($|\boldsymbol{B}| = 20$ mT). It can be seen that the conformation of MPNCs prepared at different pH values is obviously different. In fact, at pH 4.5 the NCs appear thinner and shorter in comparison with ones in higher pH solutions. The average lengths of NCs at pH 4.5, 7, and 9 are 22 μm, 25 μm, and 51 μm, respectively. Notably, the density of NCs at pH 4.5 is high and decreases with increasing pH. Additionally, it is worth noticing that the NCs at pH 4.5 are not straight and not well directed along the magnetic field direction. Their morphology is very different from that obtained in the other conditions, for which NCs are found to be well oriented and separated from each other. Consequently, through the present exploration, NCs prepared at pH 7, which are sufficiently long, dense, and well separated, were deemed to be appropriate for the fabrication of conducting wires on microelectrodes with a gap of 5 μm (Fig. S1).

The relation between pH and zeta potential of the NPs, which is shown in Fig. S2, is crucial to explain the phenomenon observed in Fig. 2. As shown in Fig. S2, the zeta potential of the NPs decreases with increasing pH value. It is important to note that the zeta potential of the glass surface also monotonically decreases as the pH value increases [21]. It was reported that formation of clusters of

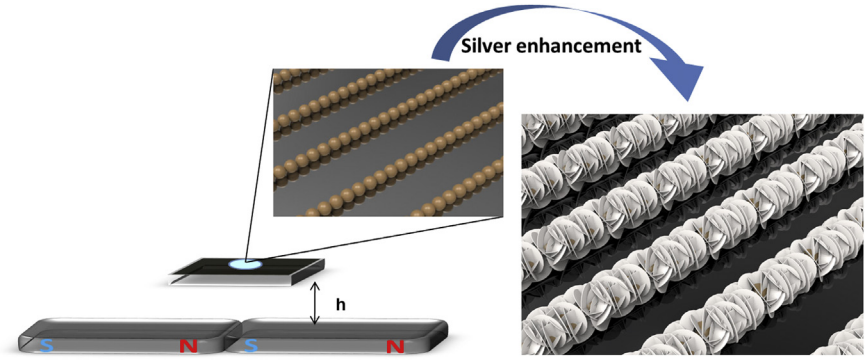

Fig. 1. Schematic illustration of magnetic-field-induced alignment of Fe_3O_4@Au NPs and silver enhancement of MPNCs.

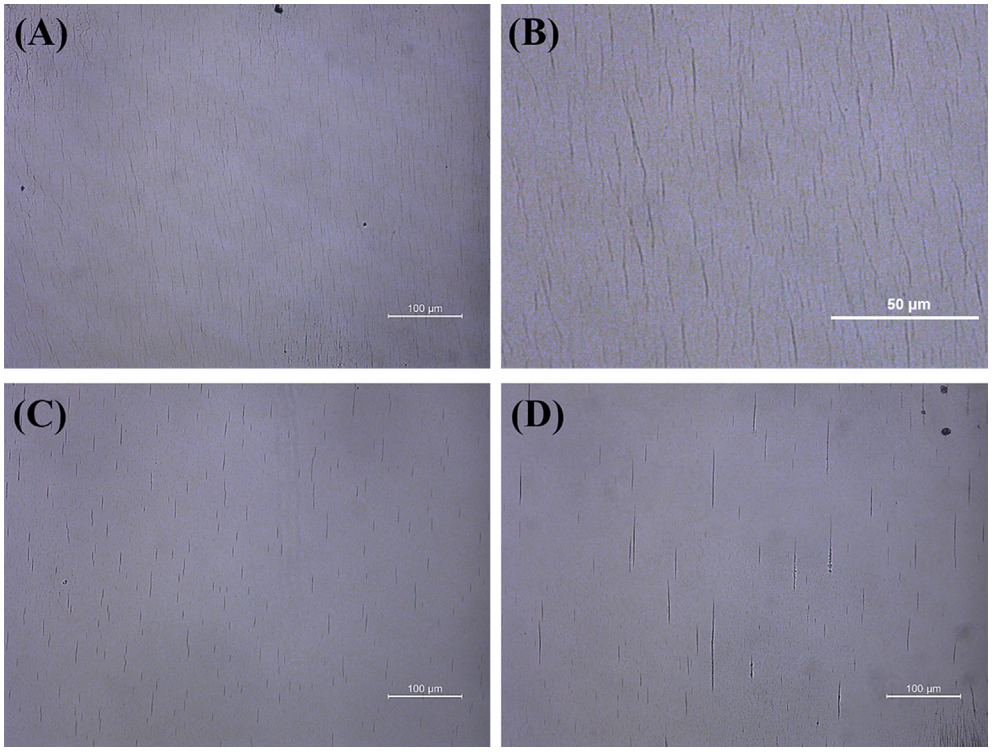

Fig. 2. Optical microscopic images of MPNCs prepared on the cover glass at different pH values: 4.5 (A–B), 7 (C), and 9 (D).

small superparamagnetic NPs, due to vdW interactions, is required for the alignment of the NPs along the magnetic field [20,22]. An increase in the absolute zeta potential of NPs, causing increased electrostatic repulsion, opposes the vdW attraction between NPs. It

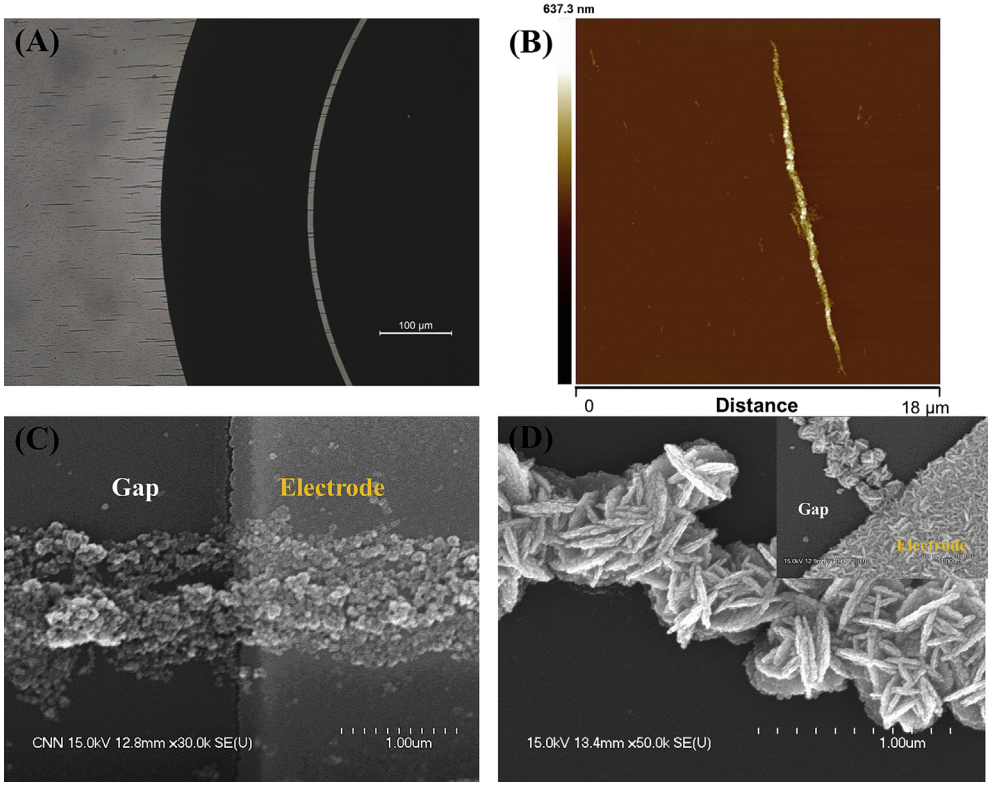

Fig. 3. Optical microscopic image of MPNCs on the electrode (A); AFM image of an MPNC (B); SEM image of junction of MPNCs with Au pad (C); silver-enhanced MPNCs (D) and their junction with Au pad (D inset).

was expected that a higher pH (higher absolute zeta potential) could lead to a reduction in the size of MPNCs. However, the opposite phenomenon is observed in Fig. 2. Therefore, there probably are other forces, besides the vdW ones, that govern the cluster formation. These forces are most likely related to the presence of a like-charged flat surface, as previous studies reported that the long-range attraction between NPs is determined by the charge density of both particles and flat surface [23,24].

3.2. Morphology of as-prepared and Ag-enhanced MPNCs

By placing the electrodes in the proper magnetic field direction, MPNCs were formed and connected two Au pads, as shown in Fig. 3A. The morphology of as-prepared MPNCs was studied by AFM and SEM measurements (Fig. 3B and C). At a micro-scale view, MPNCs display a needle shape with mean diameter of 400 nm. At higher magnification, MPNCs appear to be formed of randomly aggregated NPs as discrete building blocks (Fig. 3C). The resulting morphology of the as-prepared MPNCs is attributed to their growth mechanism [25]. Another feature worth noticing is the discontinuity of the as-prepared MPNCs. A large number of cavities were observed inside MPNCs, mainly as an effect of solvent evaporation [26].

In order to produce continuous conductive nanowires, the as-prepared MPNCs were treated with a silver enhancer using an acidic solution of hydroquinone and silver ions under low light conditions [19,27]. Silver metal is chemically deposited onto the gold particles, which act as catalysts and significantly accelerate the process. Under these experimental conditions, metal deposition only occurs along the MPNCs and on the Au pads of the microelectrode, leaving the bare glass practically clean of silver. Fig. 3D shows the morphology of silver-enhanced MPNCs treated for 20 min. The NCs show a remarkable morphology, known as nanoflowers, which are constituted of silver nanoplates. It can be observed that the nanoplates are approximately 350 nm in diameter and several tens of nanometer in thickness. Interpenetrating plates stand on each other with sharp edges, resulting in an overall spherical shape with an enlarged surface. As clearly seen, the diameter of the individual MPNPs reaches approximately up to 428 nm after enhancement (Fig. S3). In contrast to the as-prepared MPNCs, the silver-enhanced ones are continuous wires of well-connected particles. Notably, after silver enhancement, MPNCs appear to be coherently connected with the Au pad of the microelectrode (Fig. 3D inset).

3.3. Electrical properties of nanochains

As discussed above, as-prepared MPNCs are composed of discrete clusters of NPs that act as quantum wells. Quantum size effects are involved when the size of a particle is comparable to the de Broglie wavelength of the electron [28]. Under these conditions, the particles behave electronically as zero-dimensional quantum dots and are subjected to quantum-mechanical rules. Under spatial confinement, the electron energies are also quantized, which leads to various effects. Thus, electron transport in the quantized structure must be governed by quantum effects and also by the enhanced boundary scattering [29]. As a result, the I–V characteristic curve of as-prepared MPNCs shown in the inset of Fig. 4A does not follow an Ohmic behavior. High resistance and nonlinearity of as-prepared MPNCs can be also attributed to poor contact between NCs and Au pads.

As our previous study showed, the linearity and conductivity of MPNCs are significantly improved through an annealing process [16]. Accordingly, at appropriate annealing times and temperatures, coalescence occurring when Fe_3O_4@Au NPs are in contact results in the formation of larger nanoparticles. Additionally, the contact between MPNCs and Au pads was improved because of the consolidation of two objects at high temperature. As clearly seen in the inset of Fig. 4, the linearity and conductivity of annealed MPNCs were significantly improved compared with as-prepared MPNCs. However, the resistance of annealed MPNCs is still very high (~0.4×10^9 Ω compared to ~0.9×10^9 Ω for as-prepared MPNCs). Here, silver enhancement was used as an alternative to achieve a huge enhancement of conductivity of MPNCs. As shown in Fig. 4, the I–V curve of silver-enhanced MPNCs was linear, exhibiting Ohmic conductivity with low resistance (~278 Ω). Such an Ohmic response indicates continuous, metallic connections across the MPNCs. The low resistance is that expected for grain-boundary-dominated transport in a polycrystalline metal [30].

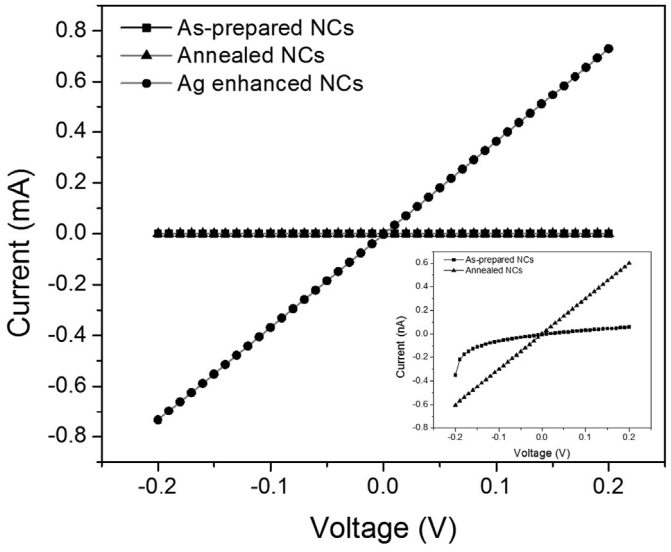

Fig. 4. I–V curves of as-prepared (solid rectangle), annealed (solid triangle), and silver-enhanced (solid circle) MPNCs. The inset shows magnified I–V curves of as-prepared and annealed MPNCs.

4. Conclusions

A simple, effective method to produce 1-D conducting materials based on magnetic-field-induced alignment of MPNPs is proposed. Continuous silver wires were obtained by treating MPNCs with a silver enhancer, resulting in an impressive enhancement of their electrical properties. The conductivity of MPNCs showed a six-fold improvement compared to that of the annealed ones. Additionally, the silver-enhanced MPNCs offer high potential for use in fascinating applications such as sensors and catalysts because of their unique surface properties.

Acknowledgements

This research was supported by the National Fisheries Research & Development Institute; from the Civil & Military Technology Cooperation Program through the National Research Foundation of Korea (NRF) (No. 2013M3C1A9055407); and from Korea-Japan International Collaboration Program through the NRF funded by the Ministry of Science, ICT & Future Planning (No. 2014K2A2A4001081).

Appendix A. Supplementary data

Supplementary data related to this article can be found at http://dx.doi.org/10.1016/j.cap.2014.11.013.

References

[1] Y. Cui, Q. Wei, H. Park, C.M. Lieber, Science 293 (2001) 1289.
[2] X. Duan, Y. Huang, Y. Cui, J. Wang, C.M. Lieber, Nature 409 (2001) 66.
[3] K. Ramanathan, M.A. Bangar, M. Yun, W. Chen, N.V. Myung, A. Mulchandani, J. Am. Chem. Soc. 127 (2005) 496.
[4] B. Kannan, D.E. Williams, C. Laslau, J. Travas-Sejdic, Biosens. Bioelectron. 35 (2012) 258.
[5] V. Rodrigues, T. Fuhrer, D. Ugarte, Phys. Rev. Lett. 85 (2000) 4124.
[6] M. Yun, N.V. Myung, R.P. Vasquez, C. Lee, E. Menke, R.M. Penner, Nano Lett. 4 (2004) 419.
[7] S. Aravamudhan, A. Kumar, S. Mohapatra, S. Bhansali, Biosens. Bioelectron. 22 (2007) 2289.
[8] S.H. Ko, I. Park, H. Pan, C.P. Grigoropoulos, A.P. Pisano, C.K. Luscombe, J.M. Fréchet, Nano Lett. 7 (2007) 1869.
[9] B. Basnar, Y. Weizmann, Z. Cheglakov, I. Willner, Adv. Mater. 18 (2006) 713.
[10] K. Nielsch, F. Müller, A.P. Li, U. Gösele, Adv. Mater. 12 (2000) 582.
[11] H. Wang, Q.W. Chen, L.X. Sun, H.p. Qi, X. Yang, S. Zhou, J. Xiong, Langmuir 25 (2009) 7135.
[12] M. Motornov, S.Z. Malynych, D.S. Pippalla, B. Zdyrko, H. Royter, Y. Roiter, M. Kahabka, A. Tokarev, I. Tokarev, E. Zhulina, Nano Lett. 12 (2012) 3814.
[13] H.D. Tran, D. Li, R.B. Kaner, Adv. Mater. 21 (2009) 1487.
[14] D. Ho, S.A.M. Peerzade, T. Becker, S.I. Hodgetts, A.R. Harvey, G.W. Plant, R.C. Woodward, I. Luzinov, T.G.S. Pierre, K.S. Iyer, Chem. Commun. 49 (2013) 7138.
[15] H. Zhou, J.-P. Kim, J.H. Bahng, N.A. Kotov, J. Lee, Adv. Funct. Mater. 24 (2014) 1439.
[16] V.T. Tran, H. Zhou, S. Kim, J. Lee, J. Kim, F. Zou, J. Kim, J.Y. Park, J. Lee, Sens. Actuat. B-Chem. 203 (2014) 817–823.
[17] H. Zhou, J. Lee, T.J. Park, S.J. Lee, J.Y. Park, J. Lee, Sens. Actuat. B-Chem. 163 (2012) 224.
[18] E. Braun, Y. Eichen, U. Sivan, G. Ben-Yoseph, Nature 391 (1998) 775.
[19] G.B. Birrell, D.L. Habliston, K.K. Hedberg, O.H. Griffith, J. Histochem. Cytochem 34 (1986) 339.
[20] Y. Lalatonne, J. Richardi, M.P. Pileni, Nat. Mater. 3 (2004) 121.
[21] Y. Gu, D. Li, J. Colloid Interface Sci. 226 (2000) 328.
[22] S. Ghosh, I.K. Puri, Soft Matter 9 (2013) 2024.
[23] J.E. Sader, D.Y. Chan, Langmuir 16 (2000) 324.
[24] T.M. Squires, M.P. Brenner, Phys. Rev. Lett. 85 (2000) 4976.
[25] W.X. Fang, Z.H. He, X.Q. Xu, Z.Q. Mao, H. Shen, EPL Europhys. Lett. 77 (2007) 68004.
[26] J. Sun, X. Liu, J. Huang, L. Song, Z. Chen, H. Liu, Y. Li, Y. Zhang, N. Gu, Sci. Rep. 4 (2014).
[27] C.S. Holgate, P.E.T.E. Jackson, P.N. Cowen, C.C. Bird, J. Histochem. Cytochem. 31 (1983) 938.
[28] M. Brust, C.J. Kiely, Colloids Surf. A 202 (2002) 175.
[29] H. Li, X.Q. Zhang, F.W. Sun, Y.F. Li, K.M. Liew, X.Q. He, J. Appl. Phys. 102 (2007) 013702.
[30] T. Scheibel, R. Parthasarathy, G. Sawicki, X.M. Lin, H. Jaeger, S.L. Lindquist, Proc. Natl. Acad. Sci. 100 (2003) 4527.